P1.13

GROUND-BASED REMOTELY SENSED HIGH TEMPORAL-RESOLUTION STABILITY INDICES ASSOCIATED WITH SOUTHERN GREAT PLAINS TORNADO OUTBREAKS

Timothy J. Wagner*, Wayne F. Feltz, Ralph Petersen, Steven A. Ackerman

Cooperative Institute for Meteorological Satellite Studies/Space Science and Engineering Center
University of Wisconsin--Madison, Madison, Wisconsin.

1. INTRODUCTION

Climatologies of stability indices associated with tornadic environments have been produced using radiosonde launches (e.g. Rasmussen and Blanchard 1998) or numerical weather prediction data (e.g. Thompson et al. 2003). The coarse temporal resolution of these datasets prevents any analysis of the finescale evolution of the pre-storm environment.

The Atmospheric Emitted Radiance Interferometer (AERI: Knuteson et al., 2004) is a ground-based infrared radiometer, was designed to measure surface incident radiation as part of the Department of Energy's Atmospheric Radiation Measurement (ARM) program (Stokes and Schwartz, 1994). Through a physical retrieval process (Smith et al. 1999), the AERI is capable of observing vertical profiles of temperature and moisture in the lowest three kilometers of the troposphere at a temporal resolution of better than 10 minutes. At higher altitudes, the AERI profiles are blended with Rapid Update Cycle-2 (RUC-2) numerical weather output to produce a profile for the entire atmospheric depth. While the RUC-2 data is of a coarser resolution than the AERI, much of the evolution of the evolution of the thermodynamic state occurs at the lower levels that AERI captures. AERI retrievals of temperature and moisture profiles have been shown to be well-correlated with coincident radiosonde launches (Feltz et al. 1998, 2003).

From late 1999 through 2003, AERI units were collocated near NOAA Profiler Network (NPN) 404 MHz radar wind profilers at five ARM Southern Great Plains (ARM-SGP) sites in Oklahoma and Kansas (Chadwick and Hassel, 1987). The wind profilers observe the three components of the wind vector at better than six minute temporal resolution. Together, these two instruments

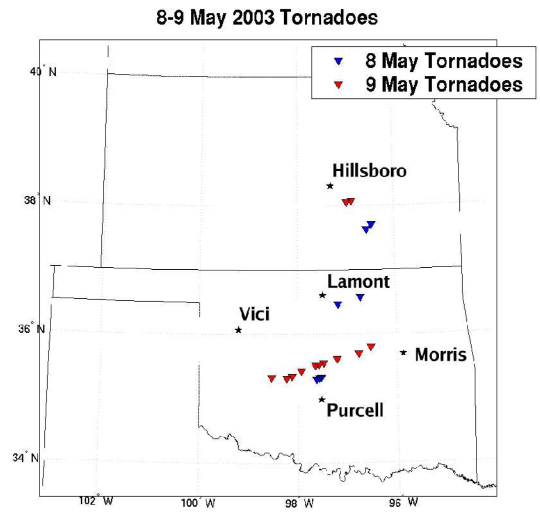

Figure 1: Map of AERI locations as part of the ARM-SGP program. Blue markers denote touchdown locations of tornadoes in 8 May 2003 outbreak, and red markers denote touchdowns of 9 May 2003 outbreak. These outbreaks are discussed in further detail in Section 5.

provide profiles of temperature, moisture, and wind, but with a temporal resolution that is far more fine. Four of the five sites considered in this study had both AERI and NPN installations. The fifth location had AERI separated from the profiler by a distance of 20 km. For the purposes of this investigation, these instruments are considered collocated. The locations of these sites can be seen in Figure 1.

2. METHODOLOGY

While stability indices are not the only parameter that an operational forecaster should investigate, they are important for the recognition of environments that produce severe storms (Johns and Doswell, 1992). There are three distinct classes of stability indices: (1) thermodynamic indices, which are computed using the just profiles of temperature and moisture; (2) aerodynamic indices, which are computed solely on the wind profile; and (3) hybrid indices that are combinations of the two. In this study, the

* *Corresponding author address*: Timothy J. Wagner, CIMSS/SSEC, 1225 West Dayton Street Room 1317, Madison, WI, 53706; e-mail: tjwagner2@wisc.edu.

thermodynamic indices of lifted index (LI), convective available potential energy (CAPE), and convective inhibition (CIN) were examined. The aerodynamic parameter of storm relative helicity (SRH) was investigated, as well as the hybrid indices of bulk Richardson number (BRN) and energy-helicity index (EHI).

An objective definition of tornado outbreak in the ARM-SGP domain was created for this study: Of all days in which at least one tornado touched down within 100 km of an AERI/NPN site, an outbreak occurred when the number of tornadoes on that day was at least one standard deviation above the mean number of tornado touchdowns on a tornado day. A tornado day was considered to begin at 3 AM CDT (0800 UTC) where there is a natural lull in tornadic activity. This definition led to a seven-tornado outbreak threshold, and seven separate days fulfilled this criterion. Tornado data was obtained from the SVRPLOT software (Hart, 1993) produced and updated by the Storm Prediction Center (SPC).

The stability indices were then computed from six hours before to six hours after the first touchdown of the outbreak, which allows for sufficient time to investigate the pre-outbreak environment as well as the outbreak itself. To perform these calculations, the profiler data were convolved to the time and height resolution of the AERI data. Since these instruments cannot inherently obtain storm motion, the storm motion vector in the SRH calculation is parameterized using the method described by Maddox (1976), in which the storm motion vector is 75% of the magnitude and 15 degrees to the right of the mean of the wind vectors at the surface, 850, 700, 500, 300, and 200 hPa.

Because the AERI is an infrared instrument, it is unable to properly compute radiances when low clouds or precipitation is above the observing site. Therefore, there are frequently gaps in the data record. The wind profilers are also susceptible to missing observations, again frequently due to precipitation. However, even with the gaps, far more observations are available than with standard synoptic rawinsonde observations. Due to the environments that typically produce supercells, the pre-storm environment for tornado outbreaks in the southern great plains is frequently clear.

3. CLIMATOLOGIES

Stability parameters were calculated for all AERI and profiler observations of the environment associated with the outbreaks. Mean values across all outbreaks and all sites were obtained. Data are presented in half-hour intervals, where each point represents the mean between the observation closest to that time point, the observation before it, and the observation after it. This was done to lessen the influence of spurious observations and reduce the number of missing observations.

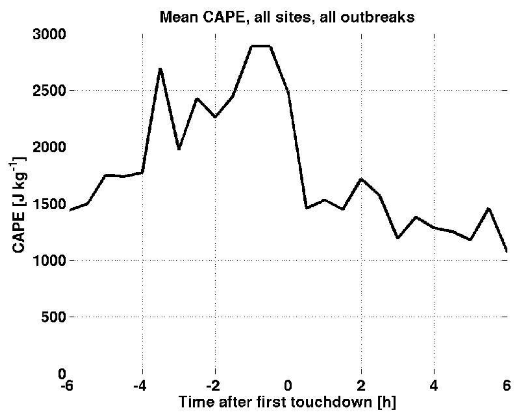

Figure 2: Five year climatology of mean Convective Available Potential Energy over all outbreaks as observed by all AERI installations. Data are presented from six hours before first tornado touchdown to six hours after first tornado touchdown.

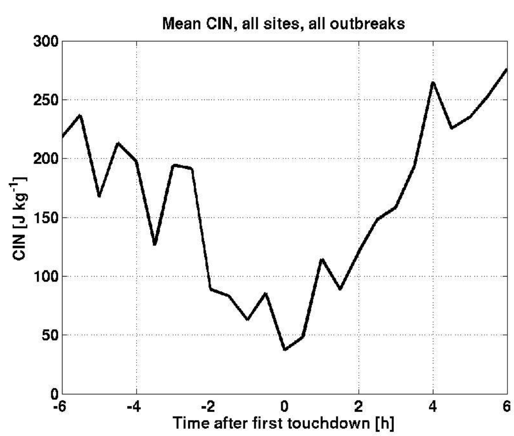

Figure 3: As in Figure 2, but for Convective Inhibition.

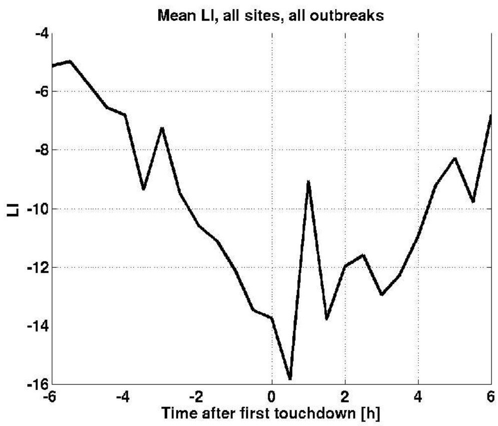

Figure 4: As in Figure 2, but for lifted index.

Because all locations have been included in these averages for this initial study, this results in a reduced amplitude for the parameters. For example, Vici, in the western part of the state of Oklahoma, may be in the post-storm environment while Morris, in the eastern portion of the state, may still be observing the pre-storm environment. No attempt was made to account for this bias. Times are normalized about time of first tornado touchdown, and extend from six hours before the first touchdown to six hours after the first touchdown. Plots of the values obtained may be seen in Figures 2 through 7.

Due to lack of low-level wind data in older observations before 2002, the climatologies for BRN, EHI, and SRH are only for four outbreaks in the years 2002 and 2003

Some general trends can be seen in the data. CAPE peaks at the time of first tornado touchdown, but LI peaks after first touchdown. A possible explanation for this is that the dependency of LI on moisture is determined near the surface, but the dependence of CAPE on moisture is determined throughout the atmosphere. As precipitation develops and tornadogenesis hastens due to baroclinic generation of vorticity in evaporatively cooled air, CAPE is depleted. The lower levels remain unmodified while the midlevels cool, resulting in an increasing LI with decreasing CAPE. Further investigation into this phenomenon is required.

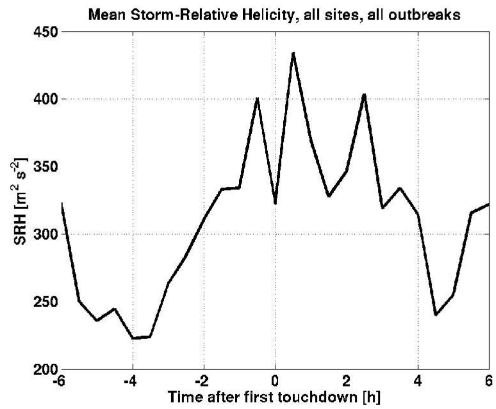

Figure 5: Five year climatology of mean SRH over all outbreaks as observed by all profilers in the AERI/NPN domain. Data are presented from six hours before first tornado touchdown to six hours after first tornado touchdown.

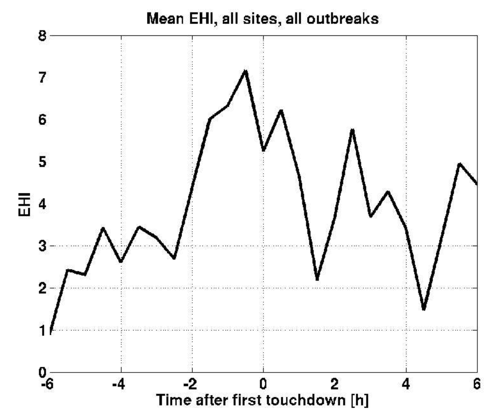

Figure 6: Mean Energy-Helicity index as observed by AERI and wind profilers for all outbreaks at all sites.

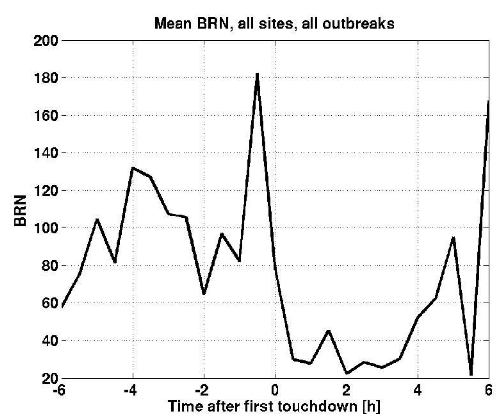

Figure 7: As in Figure 6, but for Bulk Richardson Number

4. CASE STUDIES

Two case studies chosen for examination in further detail because of their particularly continuous data record before and after tornadogenesis. 8 May and 9 May 2003 were part of an unprecedented week of tornadic activity across the United States. Both of these days featured outbreaks that were well-observed in the AERI/NPN domain, with seven tornado touchdowns on the 8th and 12 more on the 9th. The locations of these touchdowns are shown in Figure 1.

The first touchdown within the domain on 8 May was at 5:00 PM CDT (2200 UTC) near Newcastle, Oklahoma, southwest of Oklahoma City. (Other tornadoes formed earlier in the day, but they were more than 100 km away from an ARM/SGP facility.) The subsequent tornadoes stretched across the southern Oklahoma City metropolitan area. The strongest of these was classified as F4 on the Fujita scale and caused more than $350 million in damages. The final tornado touchdown of this outbreak was at 6:46 CDT (2346 UTC). These tornadoes were spawned by supercells that formed southeast of Oklahoma City. The cells then tracked off to the east-northeast.

The closest ARM-SGP site to this outbreak was Purcell, located 50 km south of Oklahoma City. Unfortunately, cloud cover for much of the day prevented the AERI at Purcell from recording observations. Therefore, data from Vici (170 km northwest of Oklahoma City) and Lamont (150 km north of Oklahoma City) are presented here in Figures 8 through 10.

The propagation of the cold front that forced the convection can easily be seen in this data. The instability measured at Vici drops well before a similar loss of instability is measured at Lamont. A time-height cross section of temperature and water vapor mixing ratio measured at Lamont is shown in Figure 11. Similar signals are visible in time-height cross sections from other sites.

The variability of the wind on short time scales is clearly visible in these individual case studies. For example, a plot of BRN shows large oscillations due to the varying nature of the low-level shear. These large swings in value are not visible in the climatologies of wind-based parameters due to the averaging.

The outbreak of 9 May covered much of the same geographical area. This outbreak was later in the day, with the first touchdown at 8:49 PM CDT (0149 UTC on 10 May 2003). The strongest tornado of this outbreak was rated as F3 on the Fujita scale, and the last tornado touched down at 3:04 AM CDT (0804 UTC) on 10 May. Plots of selected convective indices are shown in Figures 12-14.

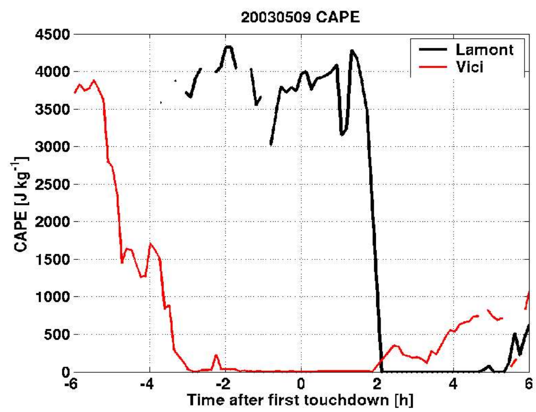

Figure 8: AERI-observed CAPE for Lamont, OK (black) and Vici, OK (red) for the tornado outbreak of 8 May 2003 from 6 hours before the first tornado touchdown to six hours after the first tornado touchdown.

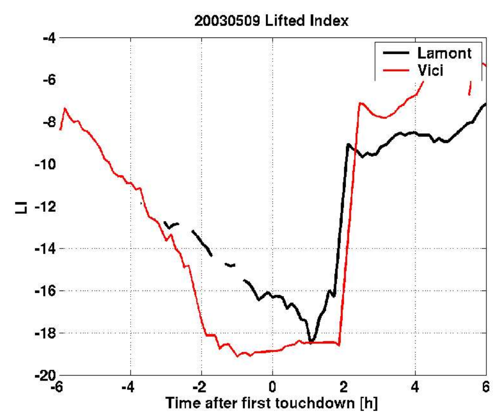

Figure 9: As in Figure 8, but for LI.

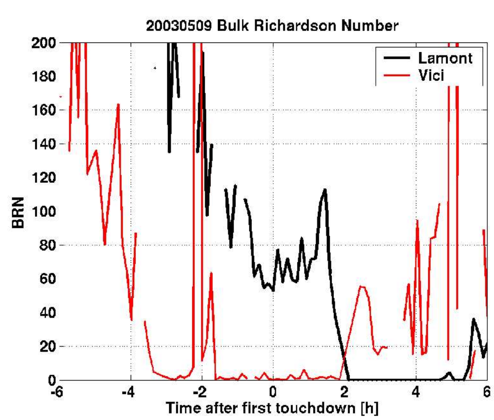

Figure 10: AERI and NPN observed Bulk Richardson Number for the Tornado outbreak on 8 May 2003.

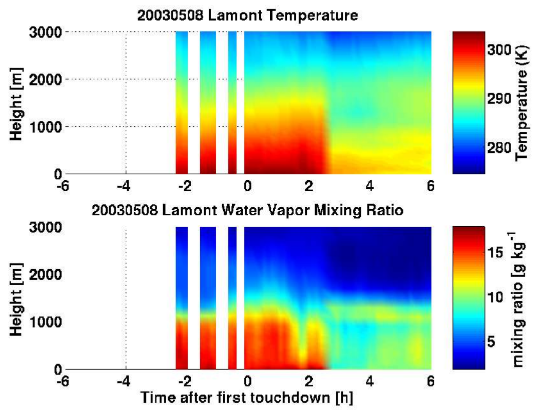

Fgure 11: Time-height cross-section of AERI observed temperature (in K) and water vapor mixing ratio (in g kg^{-1}) at Lamont for the Tornado outbreak of 8 May 2003.

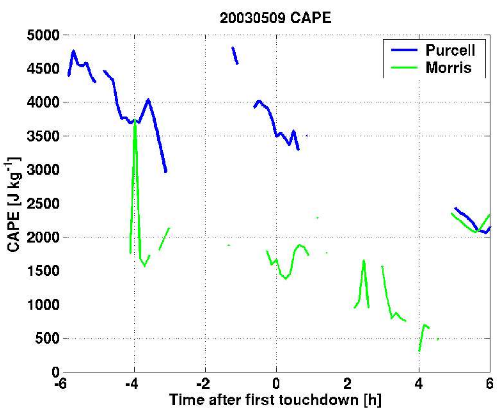

Figure 11: AERI observed CAPE for Purcell, OK (blue) and Morris, OK (green) for the tornado outbreak of 9 May 2003.

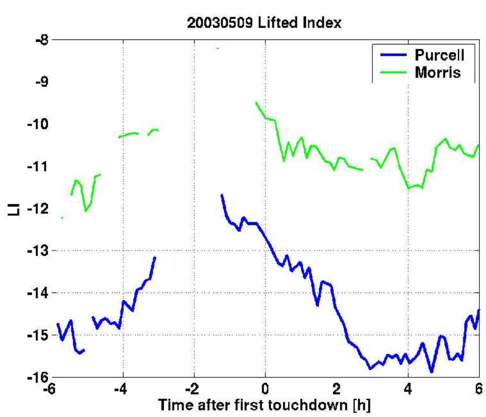

Figure 12: As in Figure 11, but for LI.

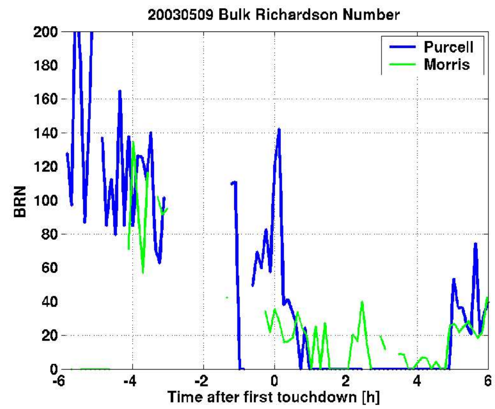

Figure 13: AERI and NPN observed Bulk Richardson Number for the Tornado outbreak on 9 May 2003.

5. CONCLUSIONS AND FUTURE PLANS

The standard radiosonde launch schedule cannot capture the finescale evolution of the pre-storm environment. Remotely sensed observations from ground based instruments such as AERI and NPN show great promise in observing the atmosphere at a finer temporal resolution than previously possible. These observations are not only useful for operational forecasting, but studies have shown that such observations increase forecast skill when assimilated into numerical weather prediction models (Benjamin et al., 2005).

An overall theme can be seen in the time-series plots of stability indices associated with tornado outbreaks: atmospheric instability tends to increase until the time of first tornadogenesis, then it decreases, but there can be significant variation from case to case. Wind shear also increases as the time of the first tornado touchdown approaches.

The authors plan to investigate if these instruments can aid in the discrimination between tornadic and non-tornadic supercells prior to tornadogenesis.

6. ACKNOWLEGEMENTS

The authors would like to thank H. Ben Howell for writing routines to convolve wind profiler observations to the AERI time and height grid. Data were obtained from the Atmospheric Radiation Measurement (ARM) Program sponsored by the U.S. Department of Energy, Office of Science, Office of Biological and Environmental Research, Environmental Sciences Division.

7. REFERENCES

Chadwick, R. B. and N. Nassel, 1987. Profiler: The next generation surface-based atmospheric sounding system. Preprints, *3rd Int'l, Conf. on Interactive Information and Processing Systems for Meteorology*, New Orleans, LA, Amer. Met. Soc., 15-21.

Feltz, W.F., W.L. Smith, R.O. Knuteson, H.E. Revercomb, H.M. Woolf, and H.B. Howell, 1998: Meteorological applications of temperature and water vapor retrievals from the ground-based atmospheric emitted radiance interferometer (AERI). *J. Appl. Meteor.,* 37, 857-875.

------, W.L. Smith, H.B. Howell, R. O. Knuteson, H. Woolf, and H. E. Revercomb, 2003: Near-continuous profiling of temperature, moisture, and atmospheric stability using the Atmospheric Emitted Radiance Interferometer (AERI). *J. Appl. Meteor.*, **42**, 584-597.

Hart, J. A., 1993: SVRPLOT: A new method of accessing and manipulating the NSSFC severe weather database. Preprints, *17th Conf. on Severe Local Storms*, St. Louis, MO, Amer. Meteor. Soc., 40-41.

Johns, R. H. and C. A. Doswell III, 1992: Severe Local Storms Forecasting. *Wea. Forecasting*, **7**, 588-612.

Knuteson, R. O. and coauthors, 2004: Atmospheric Emitted Radiance Interferometer, Part I: Instrument Design. *J. Atmos. Oceanic Technol.*, **21**, 1763-1776.

Rasmussen, E. N., and D. O. Blanchard, 1998: A baseline climatology of sounding-derived supercell and tornado forecast parameters. *Wea. Forecasting*, **13**, 1148-1164

Smith, W.L, W.F. Feltz, R.O. Knuteson, H.E. Revercomb, H.B. Howell, and H.M. Woolf, 1999: The retrieval of planetary boundary layer structure using ground-based infrared spectral radiance measurements. *J. Atmos. Oceanic Technol.,* **16,** 323-333.

Stokes, G. M. and S. E. Schwartz, 1994: The Atmospheric Radiation Measurement (ARM) program: programmatic background and design of the cloud and radiation test bed. *Bull. Amer. Meteor. Soc.*, **75**, 1201-1221.

Thompson, R. L., R. Edwards, J. A. Hart, K. L. Elmore, and P. Markowski, 2003: Close proximity soundings within supercell environments obtained from the Rapid Update Cycle. *Wea. Forecasting*, **18**, 1243-1261.